J Biol Inorg Chem (2005) 10: 550–563
DOI 10.1007/s00775-005-0001-9

ORIGINAL ARTICLE

Enrico G. Funhoff · Thyra E. de Jongh
Bruce A. Averill

Direct observation of multiple protonation states in recombinant human purple acid phosphatase

Received: 18 December 2004 / Accepted: 25 May 2005 / Published online: 11 August 2005

Abstract To date, most spectroscopic studies on mammalian purple acid phosphatases (PAPs) have been performed at a single pH, typically pH 5. The catalytic activity of these enzymes is, however, pH dependent, with optimal pH values of 5.5–6.2 (depending on the form). For example, the pH optimum of PAPs isolated as single polypeptides is around pH 5.5, which is substantially lower that of proteolytically cleaved PAPs (ca. pH 6.2). In addition, the catalytic activity of single polypeptide PAPs at their optimal pH values is four to fivefold lower than that of the proteolytically cleaved enzymes. In order to elucidate the chemical basis for the pH dependence of these enzymes, the spectroscopic properties of both the single polypeptide and proteolytically cleaved forms of recombinant human PAP (recHPAP) and their complexes with inhibitory anions have been examined over the pH range 4 to 8. The EPR spectra of both forms of recHPAP are pH dependent and show the presence of three species: an inactive low pH form ($pH < pK_{a,1}$), an active form ($pK_{a,1} < pH < pK_{a,2}$), and an inactive high pH form ($pH > pK_{a,2}$). The $pK_{a,1}$ values observed by EPR for the single polypeptide and proteolytically cleaved forms are similar to those previously observed in kinetics studies. The spectroscopic properties of the enzyme–phosphate complex (which should mimic the enzyme–substrate complex), the enzyme–fluoride complex, and the enzyme–fluoride–phosphate complex (which should mimic the ternary enzyme–substrate–hydroxide complex) were also examined. EPR spectra show that phosphate binds to the diiron center of the proteolytically cleaved form of the enzyme, but not to that of the single polypeptide form. EPR spectra also show that fluoride binds only to the low pH form of the enzymes, in which it presumably replaces a coordinated water molecule. The binding of fluoride and phosphate to form a ternary complex appears to be cooperative.

Keywords Purple acid phosphatase · EPR · Mechanism · Kinetics · Spectroscopy

Abbreviations PAP: Purple acid phosphatase · recHPAP: Recombinant purple acid phosphatase from human placenta · recRPAP: Recombinant purple acid phosphatase from rat bone · Uf: Purple acid phosphatase from pig uterine fluids · BSPAP: Purple acid phosphatase from bovine spleen · PP1: Protein phosphatase 1 · PP2B: Calcineurin · *p*-NPP: *para*-nitrophenylphosphate · MES: 2-[*N*-morpholino] ethanesulfonic acid · HEPES: (*N*-[2-hydroxyethyl] piperazine-*N*′-[2-ethanesulfonic acid]) · BSA: Bovine serum albumine · EPR: Electron paramagnetic resonance

Electronic Supplementary Material Supplementary material is available for this article at http://dx.doi.org/10.1007/s00775-005-0001-9

E. G. Funhoff · T. E. de Jongh
Swammerdam Institute for Life Sciences,
University of Amsterdam, Plantage Muidergracht 12,
1018 Amsterdam, The Netherlands

B. A. Averill (✉)
Department of Chemistry, University of Toledo,
2801 West Bancroft Road, Toledo,
OH, 43606-3390 USA
E-mail: baa@utoledo.edu
Tel.: +1-419-530-1585
Fax: +1-419-5301586

E. G. Funhoff
Institute of Biotechnology, ETH Hönggerberg,
Zürich, Switzerland

Introduction

Purple acid phosphatase (PAP)[(a)], also known as tartrate-resistant acid phosphatase (EC 3.1.3.2.) or type 5 acid phosphatase, is a member of the αβ-hydrolase family. The presence of a mixed-valent dinuclear non-heme iron center at the active site places it in the larger

family of non-heme diiron enzymes, such as methane monooxygenase, ribonucleotide reductase, and hemerythrin [1–3]. To date, research has centered on the elucidation of the active site structure of PAP. With the publication of X-ray structure determinations of the PAPs from kidney bean (KBPAP) [4, 5], sweet potato [6], porcine uterine fluids (uteroferrin, Uf) [7, 8], and rat bone (recRPAP) [9, 10], the focus of attention has turned to the physiological function of these enzymes [11, 12]. Mammalian PAPs exhibit a broad and non-specific phosphatase activity towards phosphoproteins [13, 14], and they are also able to perform Fenton-type chemistry [15–17]. PAPs have been proposed to be involved in the transport of iron in fetal pigs [18, 19], in osteoporosis [20, 21], in the immune response [22–24], and possibly in pathological processes such as Alzheimer's disease [25]. Although the cDNA sequence indicates that the mammalian enzymes are translated as single polypeptide proteins [26], purification often yields a proteolytically cleaved enzyme that consists of two non-covalently linked fragments with masses of ca. 20 and 16 kDa, respectively [13, 27]. The proteolytically cleaved form differs from the single polypeptide form in catalytic activity, pH optimum, and characteristic EPR spectrum at pH 5.0 [13, 28], due primarily to the absence of an interaction between an aspartate residue in an exposed peptide loop and the active site residues [29].

Despite the availability of detailed structural information, the catalytic mechanism of PAPs remains ambiguous. Experiments with bovine spleen PAP (BSPAP) and the substrate S_p-2′,3′-methoxymethylidene-ATP-$\gamma S\gamma^{18}$ $O\gamma^{17}$ O containing a chiral phosphate group showed that the hydrolysis results in net inversion of configuration at phosphorus [30], ruling out the mechanism with a phosphoenzyme intermediate that had been proposed earlier [31] and supporting a mechanism in which the substrate is directly attacked by water. The mode of coordination of the substrate in the active enzyme is not known, nor is the identity of the water/hydroxide that acts as the nucleophile. Possibilities for the latter include: (1) a terminally bound Fe^{3+} hydroxide; (2) a hydroxide bridging the Fe^{3+} and Fe^{2+} ions; (3) a terminally bound Fe^{2+} hydroxide; and (4) a water/hydroxide molecule in the second coordination sphere (Fig. 1) [32]. The absence of burst kinetics for BSPAP at pH 7 has been interpreted in terms of a model in which the hydrolysis of the phosphate ester is the rate limiting step, rather than the release of phosphate [32].

Because it is assumed to mimic the binding mode of the substrate, phosphate has been used extensively as a substrate analogue. Several kinetics [33, 34] and spectroscopic studies at pH 5 (e.g., Mössbauer [35], NMR [36], EPR [34], EXAFS [37], and CD/MCD [38]) have shown that phosphate is a competitive inhibitor of the enzyme and that it binds in a bidentate fashion to the two metal ions. Merkx et al. [32] however, showed that these studies were performed at a pH that is well below the optimal pH for enzymatic activity and proposed that at the pH optimum phosphate binds in a monodentate fashion to the Fe^{2+} site. X-ray structures of recRPAP crystallized at pH 7 [10], and λ phage protein phosphatase [39], in which the active site residues are almost identical to those of PAP [40], with sulfate bound to the binuclear site support this proposal. It should be noted, however, that in both protein structures an inhibiting cation is present (Zn in RPAP and Hg in λPP) which may distort the active site structure, and the oxidation state of the diiron center in the recRPAP structure was not specified.

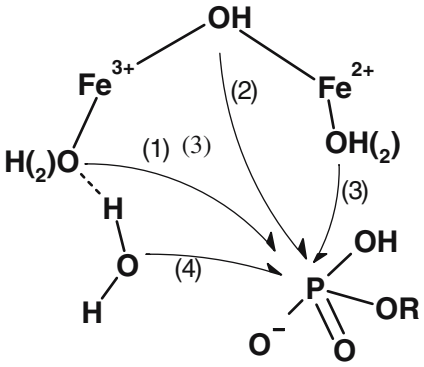

Fig. 1 Schematic representation of the dinuclear active site with the possible nucleophilic water/hydroxide. (*1*) Terminally bound Fe^{3+} hydroxide; (*2*) a hydroxide bridging the Fe^{3+} and Fe^{2+} ions; (*3*) a terminally bound Fe^{2+} hydroxide; or (*4*) a water/hydroxide molecule in the second coordination sphere

Electron paramagnetic resonance and kinetics studies, using fluoride as a hydroxide analogue and phosphate as a substrate analogue, have shown that FeZn–BSPAP forms a ternary enzyme–phosphate–fluoride complex in which fluoride presumably replaces a water/hydroxide bound to the ferric ion [41]. Based on the shift in the Fe^{3+}-μ–OH vibration of FeZn–Uf and FeZn–Uf–AsO_4 observed in the resonance Raman spectra, Que and co-workers proposed that the nucleophile is the bridging water/hydroxide. Because this shift was not observed with phosphate, however, the binding mode of phosphate, and thus of substrate, remains an open question [42]. Recent ENDOR results, which indicated the absence of a solvent molecule at the trivalent metal site [43], were interpreted in favor of the bridging hydroxide as the nucleophile although in high-resolution structures of the closely related protein phosphatases the presence of ordered solvent ligands to the Fe^{3+} site is clearly shown [44].

In the present study, we examined the pH dependence of the kinetics and spectroscopic properties of the single polypeptide and the proteolytically cleaved form of Fe^{3+} Fe^{2+}-recHPAP in the absence and presence of the substrate analogue phosphate and the hydroxide analogue fluoride. The results provide new insights into the mode of coordination of these anions to the diiron site of mammalian PAPs under catalytically relevant conditions.

Materials and methods

General

Single polypeptide recHPAP was expressed by a baculovirus expression system and the reduced form was produced using a 10 L Bioflow 3000 system (New Brunswick Scientific) for large-scale production and purified. Reduced proteolytically cleaved protein was obtained by trypsin digestion, followed by Fe^{2+}/ascorbic acid reduction and size exclusion chromatography as described [28]. Enzyme concentrations were determined after centrifugation of the sample (10,000*g*) from the maximal absorbance in the UV–vis spectrum ($\lambda_{max} = 505$–550; $\epsilon = 4{,}080\ M^{-1}\ cm^{-1}$) [45] on a Cary 50 spectrophotometer.

Kinetics

All assays were performed using the fixed-point assay at 22°C [28]. The assay buffer contained 100 mM Na-acetate, 100 mM MES, or 100 mM HEPES. Enzyme dilutions were made in 50 mM MES pH 6.5, containing 2 M KCl and 0.5 mg/ml BSA. Values of K_i were determined by measuring the rate of hydrolysis of *p*-NPP, using at least six different *p*-NPP concentrations with several fixed inhibitor concentrations. Assay time was restricted to 2 min. The results were fitted to the appropriate inhibition equation using the program Leonora (Athel Cornish-Bowden, version 1.0, 1994).

pH dependence of the EPR spectrum of reduced recHPAP

Electron paramagnetic resonance spectra were obtained at 4–5 K on a X-band Bruker ECS106 EPR spectrometer equipped with an Oxford Instruments ESR900 helium-flow cryostat with an ITC4 temperature controller and a AEG magnetic field calibrator. To follow a pH titration by EPR, 150 µL of mixed-valent recHPAP was taken for each pH from an enzyme stock solution, and buffer exchanged into a buffer mix (150 mM Na-acetate, 150 mM MES, and 150 mM HEPES, 180 mM KCl, and 20% glycerol) at the appropriate pH by repetitive dilution/concentration. The pH of each sample was measured to ensure correct pH and the sample was centrifuged (10,000*g*). The enzyme concentration and its λ_{max} at this pH were determined by UV–vis spectroscopy before the sample was transferred to the EPR tube. The protein was frozen in liquid N_2.

pH dependence of the EPR spectrum of the enzyme–phosphate complex

Electron paramagnetic resonance samples containing reduced recHPAP were thawed and made anaerobic by repetitive vacuum/flushing with argon. From anaerobic stock solutions of phosphate, prepared at the correct pH to avoid changes in sample pH, phosphate was added under anaerobic conditions to a concentration of 50 mM and the samples were frozen in liquid N_2 immediately after mixing. After recording the EPR spectrum, the sample was thawed and λ_{max} and its concentration were determined within a minute by measuring its UV–vis spectrum. No protein denaturation was observed.

pH dependence of the EPR spectrum of the enzyme–fluoride and enzyme–fluoride–phosphate complex

Reduced samples of recHPAP were buffer exchanged to the appropriate pH in a buffer containing 150 mM Na-acetate, 150 mM MES, 150 mM HEPES, 180 mM KCl, and 20% glycerol, and EPR spectra were recorded. After thawing, the samples were made 10 mM in fluoride using stock solutions, visible spectra were recorded and the samples were frozen in liquid N_2. After recording the EPR spectra, the samples were thawed and made anaerobic, and phosphate was added from an anaerobic stock solution that had been adjusted to the destined pH, to give concentrations of 50 mM. After again recording the EPR spectra, the samples were thawed and UV–vis spectra were recorded within a minute at thawing. UV–vis spectra and centrifugation did not show enzyme denaturation during all EPR experiments.

Analysis of EPR spectra

The spectra were analyzed using the programs SAE02, SAE03, and SAE15, programs developed by Dr. S.P.J. Albracht (Swammerdam Institute of Life Sciences). The major species of single polypeptide PAP EPR spectra at pH 5.6 and 8.0 and the species of the cleaved PAP at pH 4.0 were simulated using the program SAE15. Summation of varying ratios of these three simulated features resulted in measured spectra, verifying the assumption that all spectra of both single polypeptide recHPAP and cleaved recHPAP can in fact be explained in terms of a summation of three distinct EPR-spectra in ratios depending on pH.

To determine pK_a values from the EPR spectra of native enzyme and the enzyme–phosphate complex, spectra were analyzed using the following procedure. The signal height of the corrected signals at $g_z = 1.97$, $g_z = 1.94$, $g_z = 1.86$ were determined. These intensities were made relative by plotting them to the constant signal height of the $g = 1.73$ feature. The relative intensities were then adjusted to range from 0 to 1. For the determination of the $pK_{a,1}$ of the phosphate complex the total signal intensity was used because the $g_z = 1.86$ feature was not detectable. These data were

fitted to the Henderson–Hasselbalch equation to extract a value for pK_a using the program Igor Pro (Wavemetrics). Errors of pK_a values were maximal 0.2 pH units.

Results

pH dependence of single polypeptide and proteolytically cleaved recHPAP

Earlier studies on the single polypeptide and proteolytically cleaved forms of recHPAP showed that upon proteolysis the characteristic EPR spectrum at pH 5.0 changes from a rhombic signal with features at $g_{xyz} = 1.58,\ 1.73,\ 1.94$ into a more axial signal with features at $g_{xyz} = 1.58,\ 1.73,\ 1.86$. Reported g-values throughout the text are apparent g-values, unless stated otherwise. Together with this change, a shift in $pK_{a,1}$ was observed in the k_{cat} versus pH optimum [28]. To gain more insight into the origin of the pH dependence, we have measured the EPR spectrum of single polypeptide recHPAP over the pH range 4.0–8.0. Figure 2a shows that as the pH is increased from 4.0 to 8.0, three different species are observed, with $g_{xyz} = 1.58,\ 1.73,\ 1.86$; $g_{xyz} = 1.58,\ 1.73,\ 1.94$; and $g_{xyz} = 1.60,\ 1.73,\ 1.97$, respectively. With decreasing pH no additional features at $g > 2$ were observed. Simulation of the EPR spectra of the three species and summation in varying ratios confirmed the observed EPR spectra (not shown). Plotting the relative intensities of the three species (signal intensity relative to the intensity of the almost unchangeable $g_y = 1.73$ signal) versus pH (Fig. 3) shows that the intensity of the signal of the low pH species ($g_z = 1.86$) decreases as the pH increases. To extract pK_a values from the plots of Fig. 3, the data were fitted to the Henderson–Hasselbalch equation, which gave pK_a values with typical errors of ± 0.2 pH units. At pH 5.6 (near optimal pH), only one species (that with $g_z = 1.94$) is present in significant amounts, approximately 80%. The relative intensity of this species increases with increasing pH from 4.0 to 5.9 and then decreases as the pH is increased further. As the $g_z = 1.94$ signal decreases in intensity at pH > 5.5, a concomitant increase in the intensity of a species with $g_z = 1.97$ is observed. The $g_z = 1.97$ feature is observable

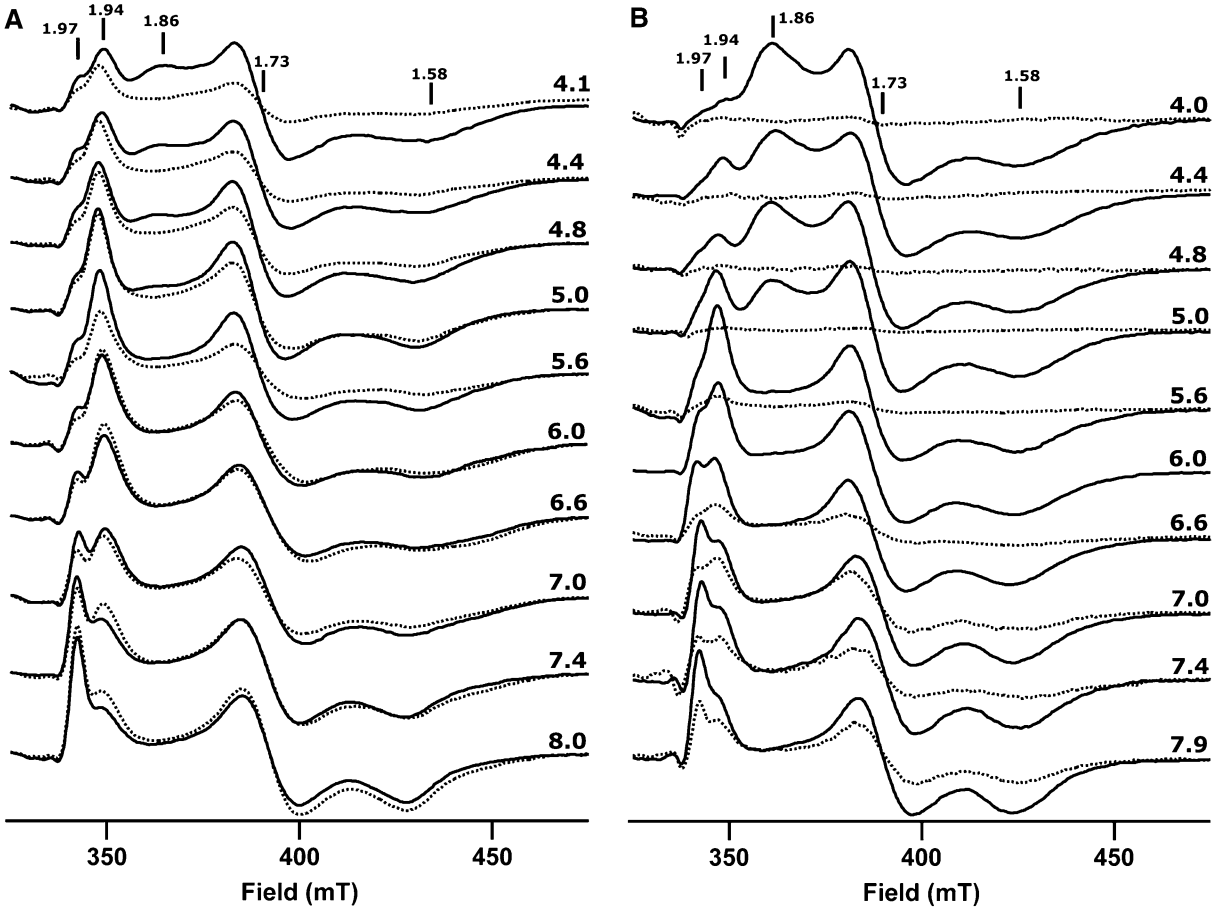

Fig. 2 Electron paramagnetic resonance spectra of native (*thick-line*) single polypeptide (**a**) and proteolytically cleaved recHPAP (**b**) over the pH range 4–8. Addition of 50 mM phosphate (*dottedline*) to the native form was performed under anaerobic conditions. All spectra were corrected for instrument gain and temperature, and the phosphate spectra were normalized using the spin concentrations of the native samples. EPR conditions: microwave power, 2 mW; microwave frequency, 9.42 GHz; modulation, 12.7 G at 100 KHz; T, 4.5–5 K

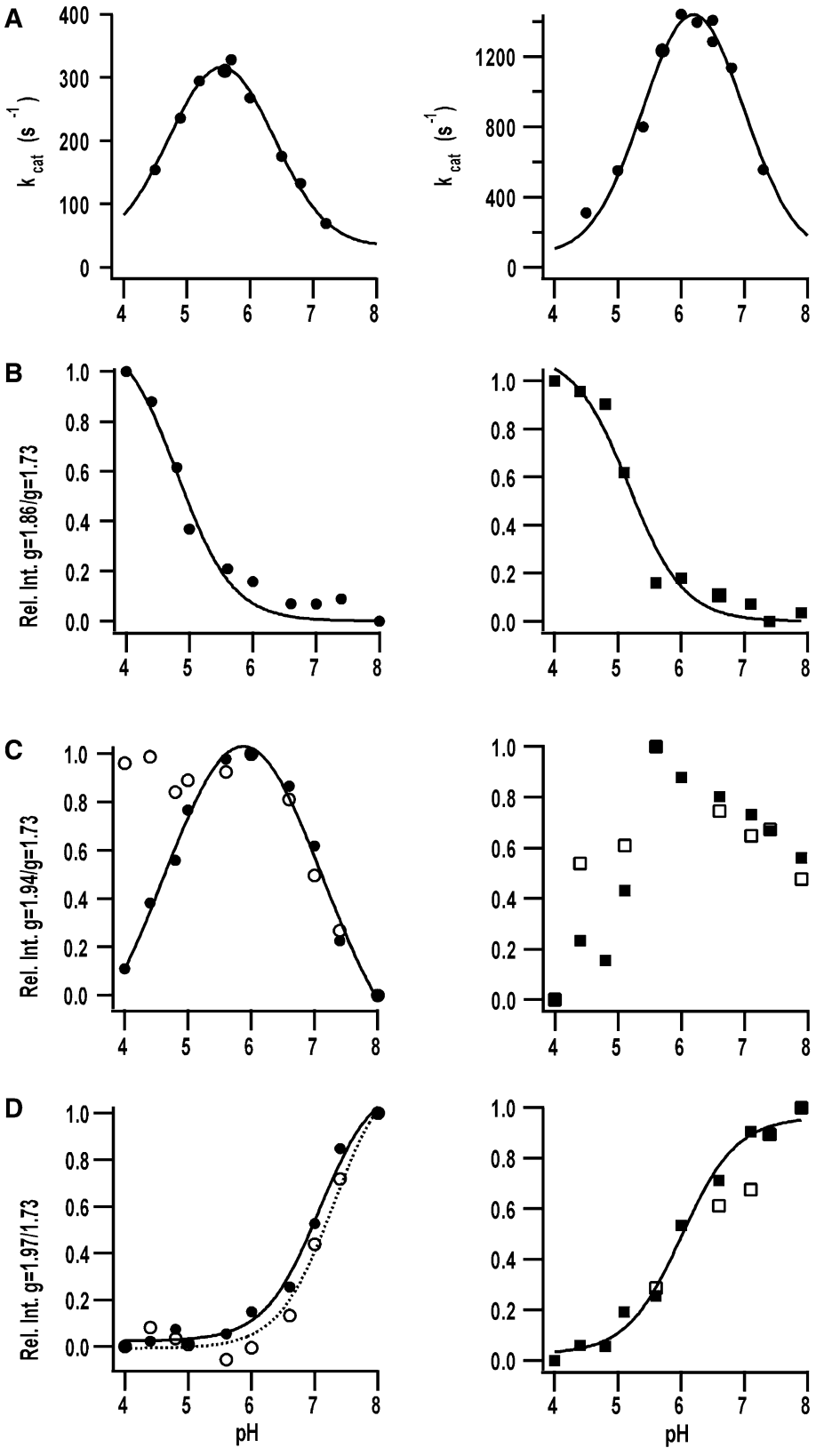

Fig. 3 Relative intensities of the EPR signals of single polypeptide (*left panel*) and proteolytically cleaved (*right panel*) recHPAP. **a** k_{cat} versus pH of recHPAP, from [27]; **b** relative intensity of the $g_z = 1.86$ signal of the native enzyme; **c** relative intensity of the $g_z = 1.94$ signal without (*closed marks*) and with (*open marks*) the presence of 50 mM phosphate; **d** relative intensity of the $g_z = 1.97$ signal without (*closed marks*) and with (*open marks*) the presence of 50 mM phosphate. To generate the figure, the relative intensity was taken as the height of the respective 1.85, 1.94 or 1.97 signals from the EPR spectra at different pH, relative to the height of the nearly constant $g_y = 1.73$ signal. All relative intensities were normalized between 0 and 1. The data of the native enzyme were fitted to the Henderson–Hasselbalch equation (*thickline*). In **d** a fitted line for the phosphate complex has also been added (*dotted line*)

as a shoulder on the $g_z = 1.94$ signal at pH values below $pK_{a,2}$. Even though kinetics studies deal with pH dependence of the enzyme–substrate complex and the EPR spectra are due to the native enzyme in the absence of substrate, the similarity of the pH dependence of both the $g_z = 1.94$ species and k_{cat} [28] (Table 1)

Table 1 Apparent pK_a values derived from kinetics and spectroscopic measurements for single polypeptide and proteolytically cleaved recHPAP

	Single polypeptide				Proteolytically cleaved			
	$pK_{a,1}$	From	$pK_{a,2}$	From	$pK_{a,1}$	From	$pK_{a,2}$	From
Kinetics								
E[a]			5.0				5.6	
E–pNPP[a]	4.6		6.7		5.5		6.9	
E–F–pNPP	~4.5–5.0		–		~5.5		–	
EPR								
E	4.6	Decr. 1.86 incr. 1.94	7.2	Decr. 1.94 incr. 1.97	5.1	Decr. 1.86 incr. 1.94	~6.8 ~6.1	Decr. 1.94 incr. 1.97
$E–PO_4$	4.5	Incr. Total s ignal intensity	7.1	Decr. 1.94 incr. 1.97	~ 6	Incr. total s signal intensity	~ 6.8	Decr. 1.94 incr. 1.97
E–F[b]	~ 4.5	Incr. 1.94	~ 7.5	Incr. 1.97	~ 5.5	Incr. 1.94	~ 7.5	Incr. 1.97
E–F–PO4[b]	–		~ 7.5	Incr. 1.97	–			

The values of these pK_a's were derived with described methods from Fig. 3. In the column accompanying the pK_a value is described from which EPR feature the value was obtained

[a]From Ref. [28]

[b]Estimated from Figs. 2, 5, and 7

strongly suggests that both are due to the same pH-dependent chemical transformations. In particular, the kinetically determined values of $pK_{es,1}$ and $pK_{es,2}$ correlate very well with the conversion of the $g_z = 1.86$ species into the $g_z = 1.94$ species and with the conversion of the $g_z = 1.94$ species into the $g_z = 1.97$, respectively.

Given the correlation between the pH dependence of the kinetics and the EPR spectra observed for the single polypeptide form of recHPAP, a similar correlation might be expected between the pH dependence of the kinetics and the EPR spectrum of the proteolytically cleaved protein, which has a $pK_{es,1}$ of 5.5 versus 4.6 for the single polypeptide form [28]. The EPR spectra of recHPAP that has been subjected to complete cleavage with trypsin are shown over the pH range 4.0–8.0 in Fig. 2b. Again, three different species are observed, with the same g_{xyz} values as for single polypeptide recHPAP. The conversion from the $g_z = 1.86$ species to the $g_z = 1.94$ species occurs at higher pH, however, in agreement with the higher pK_a values observed in the kinetics. A plot of the relative intensities of all EPR-detectable species versus pH (Fig. 3) shows that there is indeed a correlation between the pK_a values observed in kinetics and the interconversions observed by EPR for the proteolytically cleaved form of recHPAP.

The UV–vis spectra of single polypeptide and proteolytically cleaved PAP in the presence and absence of various inhibitors show a broad absorption band in the 500–560 nm region [46]. For single polypeptide PAPs (and proteolytically cleaved "low salt" BSPAP), λ_{max} is observed around 510–515 nm, while for proteolytically cleaved "high salt" BSPAP a maximum around 536 nm is reported [47]. The pH dependence of λ_{max} of both single polypeptide and proteolytically cleaved recHPAP is depicted in Fig. 4a, which shows that for the proteolytically cleaved enzyme λ_{max} shifts to higher wavelengths with decreasing pH (from 513 nm at pH 6.0 to almost 535 nm at pH 4.1). In contrast, the spectrum of the single polypeptide form exhibits almost no pH dependence: λ_{max} shifts only from 514 nm at pH 6.0 to 518 nm at pH 4.1.

Phosphate coordination

Both EXAFS studies and X-ray crystal structures of FeFe–PAP [7, 48] have shown that phosphate, a substrate analogue, coordinates to the dimetal center of oxidized PAPs in a bridging mode. In contrast, mechanistic and spectroscopic studies have been interpreted as showing that, under catalytically relevant conditions, phosphate binds to the ferrous ion of the mixed-valent diiron center [32]. In order to examine the pH dependence of phosphate coordination, the EPR spectra of the mixed valent states of both the single polypeptide and proteolytically cleaved forms of recHPAP were measured in the presence of 50 mM phosphate at various pH values under anaerobic conditions. The spectra of the enzyme in the presence of phosphate (dotted lines in Fig. 2a) show that addition of phosphate at pH 4.1–5.6 results in the loss of the $g_z = 1.86$ signal for the single polypeptide form of recHPAP. In addition, the total spin concentration decreases substantially with decreasing pH; presumably, due to partial formation of the enzyme–phosphate complex, whose relaxation properties preclude its observation under these conditions of temperature and microwave power [34, 49]. Fitting of the increase in total spin concentrations (derived from the spectra in the absence and presence of phosphate at each pH) to the Henderson–Hasselbalch equation gives an apparent pK_a of 4.6. The intensities of the $g_z = 1.94$ and $g_z = 1.97$ signals do not change upon addition of phosphate (Fig. 3), suggesting that phosphate can bind only to the $g_z = 1.86$ species in single polypeptide recHPAP, but not to the active ($g_z = 1.94$) or high pH ($g_z = 1.97$) species. As shown in Fig. 2b, the proteolytically cleaved form of recHPAP behaves dif-

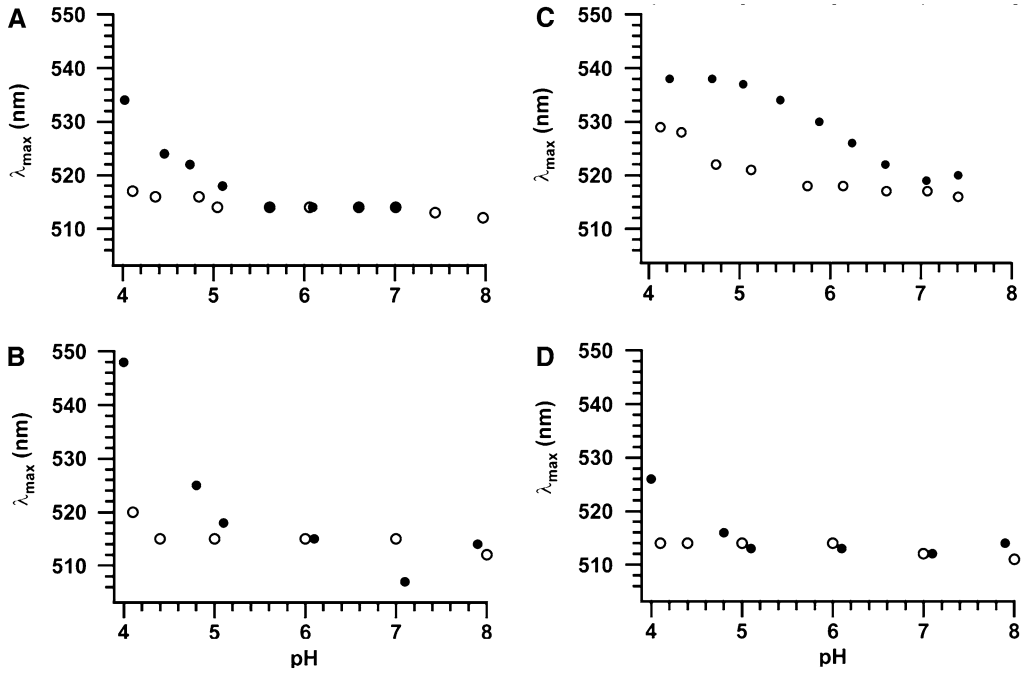

Fig. 4 pH dependence of λ_{max} of single polypeptide (*open circles*) and proteolytically cleaved (*filled circles*) recHPAP in their native state (**a**), and in the presence of 50 mM phosphate (**b**), 10 mM fluoride (**c**), and 50 mM phosphate plus 10 mM fluoride (**d**)

ferently. In this case, addition of 50 mM phosphate at pH 4.0–5.6 results in the virtual disappearance of the EPR spectra of all three species present. At higher pH values, however, both the active ($g_z = 1.94$) and high pH ($g_z = 1.97$) species can be observed even in the presence of 50 mM phosphate. At pH 7.0, addition of phosphate results in only a 40% decrease in the total spin concentration and fitting the increase in total spin concentration (before and after phosphate addition at each pH) to the Henderson–Hasselbalch equation results in an apparent pK_a of 6.0. In addition, the pH at which the $g_z = 1.94$ signal begins to decrease is 6.8 in both the native and phosphate-bound form, although for the $g_z = 1.97$ feature an apparent pK_a of 6.1 was determined.

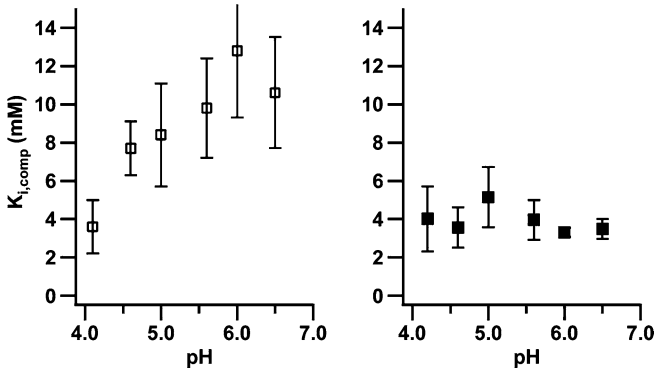

Fig. 5 Competitive inhibition constants with *errorbars* for phosphate of single polypeptide (*left panel*, *open square*) and proteolytically cleaved (*right panel*, *filled square*) recHPAP versus pH

Addition of phosphate to the reduced single polypeptide recHPAP has virtually no effect on the UV–vis spectrum (Fig. 4b). At pH values below 5, a slight increase in λ_{max} is observed, from 518 to 520 nm. For the reduced state of the proteolytically cleaved enzyme, addition of 50 mM phosphate at pH 4.0 increases λ_{max} from 534 to approximately 550 nm. No changes are observed for either the single polypeptide or proteolytically cleaved enzyme upon addition of phosphate at pH ≥5.

The pH dependence of the inhibition constants for phosphate for both the single polypeptide and proteolytically cleaved forms of recHPAP is depicted in Fig. 5. For the single polypeptide protein, k_i increases at higher pH, while for the proteolytically cleaved form no change in k_i is observed as a function of pH. At pH below 5, a K_i of 3 mM is found, and phosphate is a competitive inhibitor. Fitting the data to a mixed competitive inhibition equation gave no evidence for an uncompetitive element for either single polypeptide or proteolytically cleaved recHPAP. At higher pH, k_i increases to approximately 12 mM for the single polypeptide protein at pH 6.5. Plotting log k_i versus pH shows no evidence that deprotonation of an active site residue is coupled to phosphate binding in this pH range.

Fluoride coordination

In principle, fluoride is able to function as an analogue of the hydroxide ion. Fluoride could, therefore, replace three different groups at the diiron site in PAP; a putative terminal ferric hydroxide, a bridging hydroxide, and/or a water/hydroxide bound to the ferrous site. To study the pH dependence of binding of fluoride in EPR, 10 mM fluoride was added to single polypeptide and

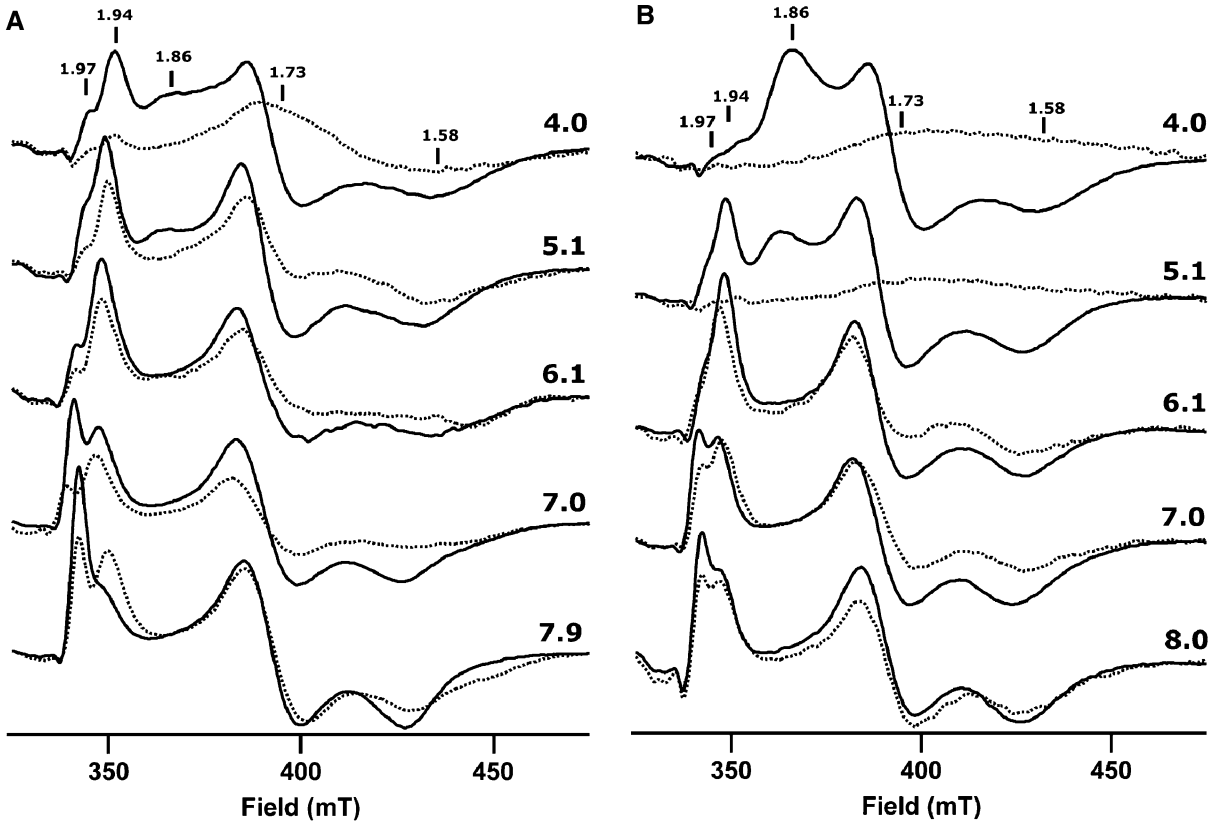

Fig. 6 EPR spectra of native (*thick line*) single polypeptide (**a**) and proteolytically cleaved recHPAP (**b**) over the pH range 4–8. 10 mM fluoride (*dotted line*) was added to the native forms. All spectra were corrected for instrument gain and temperature, and the fluoride spectra were normalized using the spin concentrations of the native samples. EPR conditions: microwave power, 2 mW; microwave frequency, 9.42 GHz; modulation, 12.7 G at 100 KHz; T, 4.5–5 K

proteolytically cleaved recHPAP at five different pH values. As shown in Fig. 6, a very broad EPR spectrum is observed at pH $< pK_{a,1}$. Above pH 5.1 for single polypeptide and pH 6.1 for proteolytically cleaved recHPAP, addition of 10 mM fluoride causes no significant changes in the EPR spectra, suggesting that fluoride does not bind to the binuclear center of either form. As with phosphate, the pH at which the added ligand perturbs the EPR spectrum of both forms is comparable to $pK_{a,1}$. This value was not determined mathematically as described for the native- and phosphate-bound forms, however, but is based on visual inspection of the intensities of the EPR features. This result strongly suggests that fluoride can replace a coordinated water molecule, but not a bound hydroxide ion, and it supports the assignment of $pK_{a,1}$ to the deprotonation of a coordinated water molecule. Thus, proton transfer events at the active site can be monitored by EPR spectroscopy. In contrast, the pH at which the $g_z = 1.94$ feature is converted into the $g_z = 1.97$ signal, which correlates with $pK_{a,2}$ in the native enzyme, is apparently affected by the presence of fluoride and shifts from approximately 7 to 7.5.

With visible spectroscopy, a shift of λ_{max} to higher wavelength is observed upon addition of fluoride at pH < 5 for single polypeptide PAP and at pH < 6.5 for the proteolytically cleaved form. The data for the λ_{max} versus pH graphs of single polypeptide and proteolytically cleaved enzyme–fluoride complex, shown in Fig. 4c, were obtained by titration of a pH 7.4 sample with HCl, rather than by measuring the visible spectra of the EPR samples.

Kinetics experiments with fluoride as inhibitor show a pH-dependent uncompetitive inhibition pattern (Fig. 7). Values of k_i are ~ 0.2 mM at pH 4–4.5 for both forms

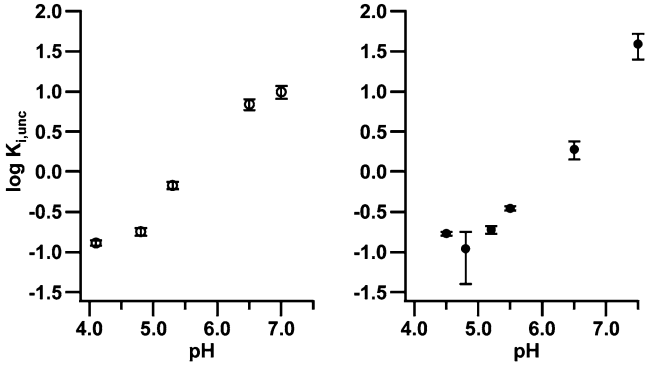

Fig. 7 Plot of the logarithm of the uncompetitive inhibition constant with error bars for fluoride versus pH for single polypeptide (*left panel*) and proteolytically cleaved (*right panel*) recHPAP

and 7 mM for single polypeptide and 2 mM for proteolytically cleaved recHPAP at pH 6.5. Plots of the logarithm of k_i versus pH show that fluoride binding to the proteolytically cleaved enzyme is independent of pH between pH 4.0 and 5.4, while a slope of approximately one is found above pH 5.4. Although, the break in the plot is not as obvious for the single polypeptide enzyme, the data are consistent with a pK_a of ~4–4.5 for single polypeptide recHPAP. At higher pH, the maximum inhibition of fluoride decreases, resulting in only 40% inhibition at pH 7.3 for single polypeptide and 20% inhibition for proteolytically cleaved recHPAP, as observed in a plot of fluoride concentration versus relative activity at 50 mM *p*-NPP (Fig. S1). When residual activity was plotted versus pH and fitted to the Henderson-Hasselbalch equation, a pK_a of 6.4 was fitted for single polypeptide recHPAP and 6.9 for proteolytically cleaved recHPAP, respectively.

The enzyme–fluoride–phosphate complex

Figure 8 shows the EPR spectra of single polypeptide and proteolytically cleaved FeFe-recHPAP as a function of pH in the presence of both 10 mM fluoride and 50 mM phosphate. Anaerobic addition of either phosphate to the enzyme–fluoride complex or fluoride to the anaerobic enzyme–phosphate complex at lower pH values results in disappearance of the EPR signal due to the formation of an EPR silent species (or a species with a very broad signal under the conditions examined). At higher pH values, however, the EPR spectra do not disappear completely. For the single polypeptide enzyme, the spectrum at pH ≥6 is that of a mixture of the $g_z = 1.94$ and 1.97 species. With proteolytically cleaved PAP, the signal due to the uncomplexed enzyme is observed above pH 7. The pH at which the 1.94 species is converted into the 1.97 species is higher in the presence of fluoride and phosphate, similar to the increase observed in the presence of fluoride alone. Separate addition of fluoride or phosphate shows that the loss of intensity is not due to oxidation of the sample, suggesting that binding of phosphate and fluoride to form a ternary complex results in a significant change in the relaxation properties of the mixed-valent diiron center.

In the visible spectra, an increase in λ_{max} is observed for the enzyme–phosphate–fluoride complex at pH < 5. As depicted in Figure 4d, this shift is most pronounced for proteolytically cleaved recHPAP

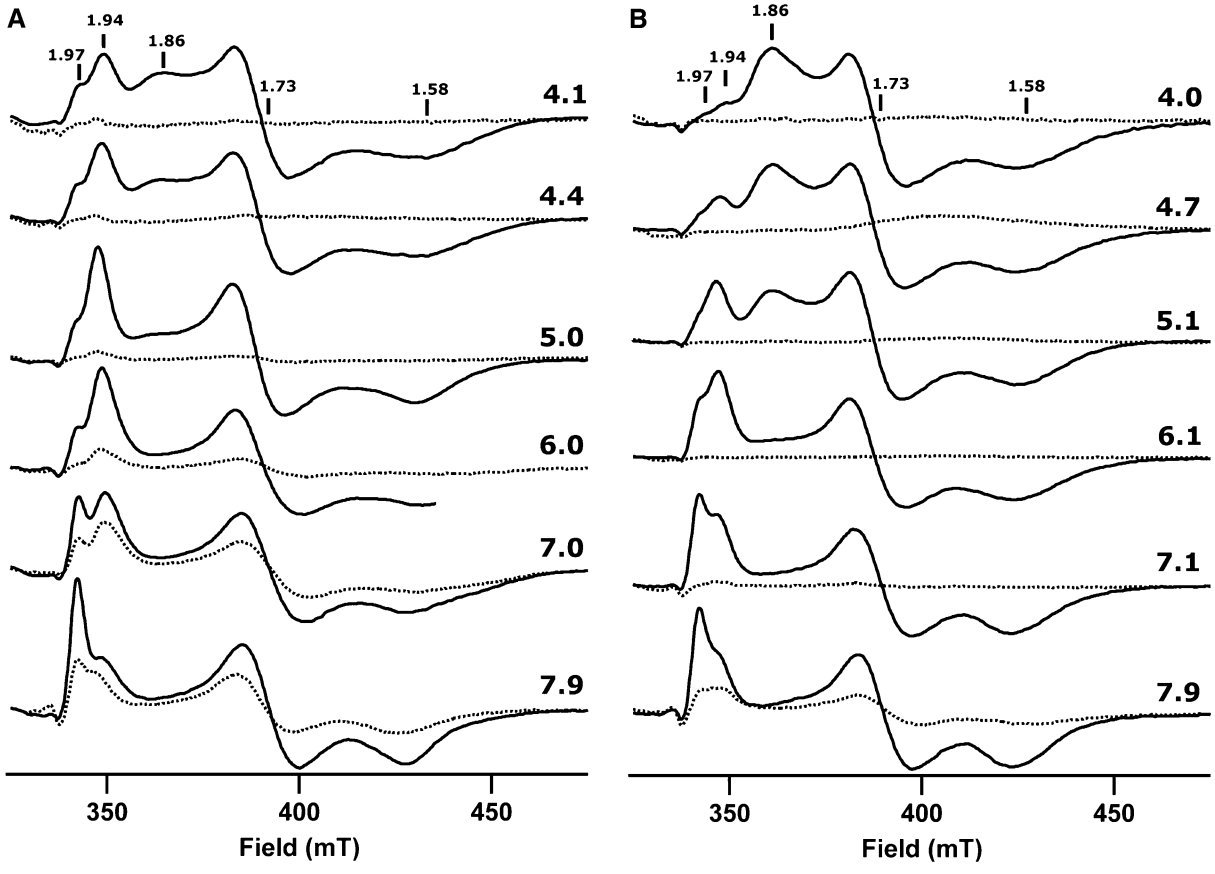

Fig. 8 Electron paramagnetic resonance spectra of single polypeptide (**a**) and proteolytically cleaved recHPAP (**b**) over the pH range 4–8 in the absence (*thickline*) and presence (*dottedline*) of 10 mM fluoride and 50 mM phosphate. All spectra were corrected for instrument gain and temperature, and the enzyme–fluoride–phosphate complex spectra were normalized using the spin concentrations of the native samples. EPR conditions: microwave power, 2 mW; microwave frequency, 9.42 GHz; modulation, 12.7 G at 100 KHz; T, 4.5–5 K

Discussion

Evidence for multiple protonation states of recHPAP

The only previous studies of the pH dependence of the EPR spectrum of a PAP were performed on proteolytically cleaved "low-salt" and "high-salt" FeFe-BSPAP over the pH range 3–7. The EPR spectrum changed from a rhombic species with $g_{xyz} = 1.65$, 1.77, 1.95 at pH 3.6 to a more axial species with $g_{xyz} = 1.59$, 1.74, 1.86 at pH 6.1. The apparent pK_a of 4.5 was attributed to the deprotonation of a metal-bound water molecule [50, 51]. Addition of phosphate gave signals with $g_{xyz} = 1.49$, 1.74, 1.91 at pH 3.6 and $g_{xyz} = 1.45$, 1.74, 1.85 at pH 6.1, whose intensity increased with increasing pH [50]. For the phosphate complex of "high-salt" BSPAP, EPR spectra showed the presence of only a single species between pH 4.5 and 7, whose intensity increased with increasing pH. The apparent pK_a of 6 [41] was substantially higher than the pK_a of 4.5 reported for the phosphate complex of the "low-salt" form, but identical to that observed in subsequent kinetic studies [32]. As previously reported, the pK_a observed by kinetics for recHPAP is shifted to higher pH by proteolysis and it has been suggested that this pK_a is due to deprotonation of a residue coordinated to the ferrous ion [28, 29]. To gain more insight into the differences in kinetics and spectroscopic characteristics of single polypeptide and proteolytically cleaved PAPs, we have examined the pH dependence of both forms of recHPAP using kinetics measurements, EPR spectrometry and visible spectroscopy over a pH range that includes both pK_a values observed in kinetics studies. We have studied both forms because two different PAPs, one a single polypeptide (Uf) and one proteolytically cleaved (BSPAP), have been extensively studied by spectroscopic methods, and we wanted to examine both forms of a single PAP to elucidate the specific effects of proteolytic cleavage.

Our results show that the three different species previously observed by EPR for PAPs from different sources [52–54] are due to three different protonation states of the enzyme (EH_2^{2+}, EH^+, and E). In the remaining part of this discussion the following notation will be used: E for the inactive high pH form ($pH > pK_{a,2}$; $g_z = 1.97$); EH^+ for the active form ($pK_{a,1} < pH < pK_{a,2}$; $g_z = 1.94$); and EH_2^{2+} for the inactive low pH form ($pH < pK_{a,1}$; $g_z = 1.86$). Somewhat surprisingly, the pH dependence of the EPR spectra correlates well with the pK_a values obtained by kinetics studies [28]. This result is unexpected, because the pK_a observed in the EPR spectra are those of the uncomplexed enzyme, while the pK_a observed in kinetics studies is that of the enzyme-substrate complex. It therefore appears as if addition of substrate results only in minor changes in the pK_a values of catalytically relevant residues. As described below, this hypothesis was tested using the substrate analogue phosphate. The proton transfer event associated with $pK_{a,1}$ also produces a shift in λ_{max}, which is more pronounced for proteolytically cleaved PAP. The proton transfer event associated with $pK_{a,2}$ is also observed in the EPR spectrum, as shown by the change in g_z from 1.94 to 1.97. The lack of a concomitant change in λ_{max}, however, suggests that the residue responsible is not a ligand to the ferric ion and suggests that protonation/deprotonation of the residue responsible for $pK_{a,2}$ results in a conformational change affecting the mixed-valent diiron site. Studies on PPs suggest that deprotonation of a conserved histidine near the dinuclear metal site (His92 in recHPAP) is responsible for $pK_{a,2}$ [55], and mutagenesis experiments suggested that this residue might be involved in base catalysis [56]. However, neither isotope effect studies nor the expected loss of the basic limb of the pH profile of mutants have been reported in support of this proposal [57–59]. Alternatively, His92 could act as a base that regenerates the metal-bound nucleophile [55, 60], but recent mutagenesis results are not consistent with such a role. They suggested that His92 is directly affected by the (de)protonation of an unknown residue, which is responsible for $pK_{a,2}$ [61]. Therefore, the observed $g_z = 1.94$–1.97 conversion in the EPR spectra might be an indirect, though coupled, EH^+ to E observation.

The interaction of recHPAP with phosphate, a substrate analog

The interaction of the substrate analogue, phosphate, with PAPs has been intensively studied. EXAFS and EPR studies of the FeZn-form [37, 42, 62] and EXAFS studies of the oxidized FeFe form [48] have suggested a bridging coordination mode for phosphate. In contrast, similar studies of a second class of inhibitory oxoanions, represented by tungstate and molybdate, suggest that they coordinate in a primarily monodentate fashion to the ferric ion [62]. In the crystal structures of KBPAP, uteroferrin, and rat bone PAP complexed with phosphate [7, 9, 63], the phosphate bridges the two metal ions in a 1,3-mode. With tungstate, a distorted bridging coordination is observed for KBPAP [63] with a slightly stronger binding to the ferric site, similar to that observed in the closely related protein phosphatases [64]. Merkx et al. [32] have argued that these studies were performed at non-optimal pH values, however, and these authors have presented data indicating that at the optimal pH of these enzymes phosphate binds to the ferrous site in a monodentate fashion [41] as suggested earlier [50]. A very recent crystal structure of sweet potato Fe^{3+} Mn^{2+} PAP at pH 3.5–4.0 showed the presence of a phosphate ion coordinated to the two metal ions in an unusual bridging tripodal mode [6].

Addition of phosphate to single polypeptide recHPAP at different pH values (Fig. 2) showed that

EH_2^{2+} binds phosphate to give a species that is effectively EPR silent [34, 49], while phosphate apparently does not bind to EH^+ and E, as was observed in a previous ^{1}H-NMR study [65]. In principle, phosphate can coordinate either in a bridging mode, replacing the presumed water/hydroxide molecules at the ferric and ferrous ions, or to the ferrous ion via replacement of the water by one phosphate oxygen atom. The lack of an observable EPR spectrum of the Uf–phosphate complex at 4 K has been attributed to extremely fast relaxation caused by the parameters J and D having comparable magnitudes, presumably due to competing exchange pathways resulting from the presence of a bridging phosphate. Recent ENDOR experiments on FeZn–Uf that showed no evidence for the presence of a water molecule at the ferric site [43] suggest that monodentate coordination of phosphate to the ferrous ion is more likely, although expanding the coordination number of the ferric ion from five to six upon phosphate coordination is also possible. In the 2.2 Å recRPAP structure [9] and in the native PP2B structure [66], however, water molecules at the ferric site could be located and refined. Thus, the presence and location of solvent molecules in and near the active site of PAPs remains unclear.

Phosphate does not appear to bind to the binuclear metal center of single polypeptide EH^+, as shown by the absence of any change in the EPR, optical, and NMR spectra [65] upon addition of phosphate. In contrast, at its optimal pH 6.3, the EPR spectrum of proteolytically cleaved recHPAP loses intensity due to partial formation of an enzyme-phosphate complex (Fig. 2). The absence of changes in λ_{max}, however, suggests that phosphate does not coordinate to the ferric ion of proteolytically cleaved EH^+ . At pH $< pK_{a,1}$, however, visible spectra clearly show that phosphate binds to the ferric site of proteolytically cleaved EH_2^{2+}, as found for the single polypeptide form. These results suggest that, at the optimal pH for activity, phosphate binds in a monodentate fashion to the ferrous site of proteolytically cleaved recHPAP. Phosphate could replace a water coordinated to the ferrous ion and mimic a non-bridging substrate molecule, as proposed by Merkx et al. [32]. The significant difference in reactivity with phosphate observed for the single polypeptide and proteolytically cleaved forms of the enzyme are difficult to rationalize if both utilize essentially the same catalytic mechanism, but may be related to the higher turnover number observed for the proteolytically cleaved form.

The interaction of recHPAP with fluoride, a hydroxide analog

To further explore the difference between single polypeptide and proteolytically cleaved recHPAP, kinetics and spectroscopic studies were performed in the presence of fluoride. Due to its ability to replace a nucleophilic water/hydroxide, fluoride inhibits a number of binuclear metalloenzymes, including urease [67], pyrophosphatases [68], and aminopeptidases [69, 70]. Inhibition of the single polypeptide and proteolytically cleaved forms of recHPAP by fluoride was found to be uncompetitive over the pH range 4–7. Hayman et al. [14] however, observed non-competitive fluoride inhibition of human PAP at pH 5.7. Fluoride has been reported to be either an uncompetitive [71], or a non-competitive inhibitor [72] of other PAPs [41, 42]. The uncompetitive inhibition observed for fluoride in this work for the EH_2^{2+} species, together with the loss of the EPR signal for both single polypeptide and proteolytically cleaved recHPAP and the minimal effect of fluoride on the absorbance maximum, suggests that fluoride replaces the coordinated water that is responsible for $pK_{a,1}$, whose deprotonation gives the nucleophilic hydroxide. Earlier, fluoride titrations of Uf at pH 4.9 monitored by EPR showed that fluoride does not bind at concentrations below 10 K_i. At higher fluoride concentrations ($> 50\times K_i$), a broad isotropic EPR spectrum was observed [73], which resembles the broad spectrum observed at low pH for single polypeptide and proteolytically cleaved recHPAP. These observations agree with our fluoride inhibition and EPR studies of the single polypeptide recHPAP: at pH 5, a k_i of 0.2 mM is found, and the EPR spectrum is significantly perturbed at this pH. Thus, fluoride can apparently replace a coordinated water molecule in the EH_2^{2+} species, but not a coordinated hydroxide ion in the EH^+ species. At pH values above $pK_{a,1}$ the lack of changes in the visible and EPR spectra of the native recHPAP enzyme strongly suggests that fluoride is not coordinating to the metal site of active EH^+, but interaction with a residue in the first or second coordination shell is possible. Thus, fluoride behaves similarly with both the single polypeptide and proteolytically cleaved forms of recHPAP. Below $pK_{a,1}$ it binds to the metal site, but at a pH where the enzyme is catalytically active it does not, as reported earlier for urease [67].

The ternary enzyme–phosphate–fluoride complex, a mimic for the active form of the enzyme during catalysis?

Although, neither phosphate nor fluoride appears to bind to the single polypeptide EH^+ enzyme, addition of both phosphate and fluoride produces a ternary enzyme–fluoride–phosphate complex, which in principle should mimic the ternary enzyme–hydroxide–substrate complex. At its optimal pH, the EPR signal of proteolytically cleaved recHPAP is abolished by addition of both fluoride and phosphate, consistent with formation of a ternary complex even though λ_{max} does not change. In "high-salt" FeZn–BSPAP and FeZn–Uf, formation of a ternary enzyme–fluoride–phosphate complex has been observed by EPR [41, 42].

Mechanistic implications

Distinguishing between the various mechanistic possibilities based on these results is difficult. Candidates for the nucleophile that attack the phosphate ester substrate include: (1) a hydroxide terminally bound to the ferric ion; (2) a hydroxide terminally bound to the ferrous ion; (3) a hydroxide bridging the two metal ions; and (4) a water in the second coordination sphere of the ferric ion. Arguments for a ferric hydroxide nucleophile include the observation that fluoride is a 50–100-fold better inhibitor of the AlZn form of BSPAP than of the FeZn or GaZn forms [74, 75], suggesting that it (and, by inference, hydroxide) interacts with the trivalent metal. Similarly, visible and EPR spectra [41] show that fluoride binding results in changes in the spectrum of the high-spin ferric ion. The following evidence, however, argues against a terminal ferric hydroxide as the nucleophile: (1) k_{cat} and pK_a do not change upon replacing the ferric ion with other metal ions [75]; (2) the EPR spectrum of FeZn-recRPAP at pH 5 does not change upon proteolysis, in contrast to the results observed for the FeFe form [28, 29]; and (3) ENDOR experiments give no evidence for coordination of a solvent molecule to the ferric ion [73].

The correlation between fluoride inhibition and the loss of the NMR signal of the enzyme–fluoride complex below $pK_{a,1}$, together with the sensitivity of $pK_{a,1}$ to perturbations at the divalent site [29, 65], suggest that the nucleophile could be the bridging hydroxide. Protonation of a bridging hydroxide, however, should dramatically decrease the exchange coupling constant *J*, resulting in greater changes in the EPR spectrum than observed here. For example, binuclear complexes containing a Ni(II)–OH–Ni(II) or Mn(II)–OH–Mn(II) unit have J values of -4.5 and $-9\ cm^{-1}$, respectively, which are decreased to $<< -2$ and $-1.7\ cm^{-1}$, respectively, upon protonation [76]. The lack of major changes in the value of *J* [76] and in the EPR spectrum [62] of proteolytically cleaved BSPAP over the pH range 3.7–5.6 also argue against the bridging hydroxide as nucleophile. The presence of a bridging carboxylate in PAPs could, however, reduce the effect of protonation of a bridging hydroxide on the exchange coupling constant. Further support for the bridging hydroxide as nucleophile comes from a recent structure of sweet potato PAP at pH 4, in which a tridentate bridging phosphate was observed [6].

This leaves either a terminal hydroxide bound to the ferrous ion or a water molecule in the second coordination sphere as the remaining candidates for the identity of the nucleophilic hydroxide. Unfortunately, several pieces of data also argue against these options. For example, the observed pK_a of 4.5 for the enzyme is almost six pH units lower than that of the hexaaquo ferrous ion ($pK_a = 10.2$), which is hard to reconcile with the pK_a of a water bound to a divalent metal ion. The large red shift in λ_{max} observed for proteolytically cleaved recHPAP at pH values below $pK_{a,1}$ suggests that protonation results in an increased positive charge on the ferric ion, which is also difficult to correlate with the protonation of a terminal hydroxide bound to the ferrous ion. However, the large red shift observed upon oxidation and the increase in λ_{max} to 525–530 nm for FeZn–BSPAP [77] show that changes at the divalent site do affect the effective positive charge on the trivalent ion. An important argument in favor of a divalently coordinated nucleophile is the dependence of the specific activity of metal-substituted forms of the enzyme upon the identity of the divalent metal ion [32, 74, 75].

The possibility that the nucleophile might be a water/hydroxide in the second coordination sphere nucleophile was put forward to rationalize the high activity of the AlZn-form of BSPAP [75], given the fact that the ligand exchange rates of Al^{3+} complexes are typically 100-fold lower than those of the corresponding Fe^{3+} complexes [78, 79]. The results presented in this study do not bear directly on this possibility. The observed change in pK_a values for His92 mutants of recRPAP to more acidic values are also consistent with this mechanistic possibility [61]. Thus, it is clear that further research using a variety of experimental approaches is necessary to resolve the problem of the identity of the nucleophilic hydroxide.

Conclusions

We have shown that three different protonation states of recHPAP can be observed by EPR and UV-vis spectroscopy. The pK_a values observed spectroscopically for the interconversion of these species correlate well with the pK_a values deduced from kinetics studies. At the optimal pH for activity, both EPR and NMR [65] spectra show that phosphate is unable to bind directly to the diiron site in single polypeptide recHPAP, raising the possibility that substrate may not bind directly to the dinuclear site during catalysis. In contrast, phosphate does bind to the ferrous site in proteolytically cleaved PAP at its optimal pH in a monodentate fashion. Kinetics studies and UV-visible and EPR spectra show that fluoride, a hydroxide analogue, can replace a coordinated water molecule, but not the nucleophilic hydroxide derived therefrom. The combination of kinetics and spectroscopic evidence now unambiguously confirmed that $pK_{a,1}$ results from the (de)protonation of this nucleophilic hydroxide and its protonation state controls the binding of inhibitory anions. In combination with our FeZn–recHAP studies [80] the bridging hydroxide, thus, seems the most likely candidate for the nucleophilic function.

Acknowledgements This research was supported by a grant from the EU Biotechnology Program (contract B104-CT-98-0385).

References

1. Lange SJ, Que L Jr (1998) Curr Opin Chem Biol 2:159–172
2. Solomon EI, Brunold TC, Davis MI, Kemsley JN, Lee S-K, Lehnert N, Nees F, Skulan AJ, Yang Y-S, Zhou J (2000) Chem Rev 100:235–349
3. Averill BA (2003) In: Que L Jr, Tolman WB (eds) Comprehensive coordination chemistry II. Elsevier, Pergamon
4. Sträter N, Klabunde T, Tucker P, Witzel H, Krebs B (1995) Science 268:1489–1492
5. Sträter N, Fröhlich R, Schiemann A, Krebs B, Körner M, Suerbaum H, Witzel H (1992) J Mol Biol 224:511–513
6. Schenk G, Gahan LR, Carrington LE, Mitic N, Valizadeh M, Hamilton SE, de Jersey J, Guddat LW (2005) Proc Natl Acad Sci USA 102:273–278
7. Guddat LW, McAlpine AS, Hume D, Hamilton S, de Jersey J, Martin JL (1999) Structure 7:757–767
8. Guddat LW, McAlpine AS, Hume D, de Jersey J, Hamilton SE, Martin JL (1999) Acta Crystal D 55:1462–1464
9. Uppenberg J, Lindqvist F, Svensson C, EkRylander B, Andersson G (1999) J Mol Biol 290:201–211
10. Lindqvist Y, Johansson E, Kaija H, Vihko P, Schneider G (1999) J Mol Biol 291:135–147
11. Oddie GW, Schenk G, Angel NZ, Walsh N, Guddat LW, DeJersey J, Cassady AI, Hamilton SE, Hume DA (2000) Bone 27:575–584
12. Andersson G, Ek-Rylander B, Hollberg K, Ljusberg-Sjoelander J, Lang P, Norgard M, Wang Y, Zhang S-J (2003) J Bone Min Res 18:1912–1915
13. Ljusberg J, EkRylander B, Andersson G (1999) Biochem J 343:63–69
14. Hayman AR, Warburton MJ, Pringle JAS, Coles B, Chambers TJ (1989) Biochem J 261:601–609
15. Sibille J-C, Doi K, Aisen P (1987) J Biol Chem 262:59–62
16. Ylipahkala H, Halleen JM, Kaija H, Vihko P, Vaananen HK (2003) Biochem Biophys Res Comm 308:320–324
17. Halleen JM, Raisanen SR, Alatalo SL, Vaananen HK (2003) J Bone Min Res 18:1908–1911
18. Nuttleman PR, Roberts RM (1990) J Biol Chem 265:12192–12199
19. Buhi WC, Ducsay CA, Bazer FW, Roberts RM (1982) J Biol Chem 257:1712–1723
20. Hayman AR, Jones SJ, Boyde A, Foster D, Colledge WH, Carlton MB, Evans MJ, Cox TM (1996) Development 122:3151–3162
21. Angel NZ, Walsh N, Forwood MR, Ostrowski MC, Cassady AI, Hume DA (2000) J Bone Min Res 15:103–110
22. Hayman AR, Bune AJ, Bradley JR, Rashbass J, Cox TM (2000) J Histochem Cytochem 48:219–227
23. Ashkar S, Weber GF, Panoutsakopoulou V, Sanchirico ME, Jansson M, Zawaideh S, Rittling SR, Denhardt DT, Glimcher MJ, Cantor H (2000) Science 287:860–864
24. Bune AJ, Hayman AR, Evans MJ, Cox TM (2001) Immunology 102:103–113
25. Lang P, Schultzberg M, Andersson G (2001) J Histochem Cytochem 49:379–396
26. Lord DK, Cross NCP, Bevilacqua MA, Rider SH, Gorman PA, Groves AV, Moss DW, Sheer D, Cox TM (1990) Eur J Biochem 189:287–293
27. Orlando JL, Zirino T, Quirk BJ, Averill BA (1993) Biochemistry 32:8120–8129
28. Funhoff EG, Klaassen CHW, Samyn B, Van Beeumen J, Averill BA (2001) Chem Bio Chem 2:355–363
29. Funhoff EG, Ljusberg J, Wang Y, Andersson G, Averill BA (2001) Biochemistry 40:11614–11622
30. Mueller EG, Crowder MW, Averill BA, Knowles JR (1993) J Am Chem Soc 115:2974–2975
31. Vincent JB, Crowder MW, Averill BA (1991) J Biol Chem 266:17737–17740
32. Merkx M, Pinkse MWH, Averill BA (1999) Biochemistry 38:9914–9925
33. Pyrz JW, Sage JT, Debrunner PG, Que L Jr (1986) J Biol Chem 261:11015–11020
34. David SS, Que L Jr (1990) J Am Chem Soc 112:6455–6463
35. Sage JT, Xia Y-M, Debrunner PG, Keough DT, de Jersey J, Zerner B (1989) J Am Chem Soc 111:7239–7247
36. Wang Z, Ming L-J, Que L Jr, Vincent JB, Crowder MW, Averill BA (1992) Biochemistry 31:5263–5268
37. Wang X, Randall CR, True AE, Que L Jr (1996) Biochemistry 35:13946–13954
38. Yang YS, McCormick JM, Solomon EI (1997) J Am Chem Soc 119:11832–11842
39. Voegtli WC, White DJ, Reiter NJ, Rusnak F, Rosenzweig AC (2000) Biochemistry 39:15365–15374
40. Vincent JB, Averill BA (1990) FEBS J 263:265–268
41. Pinkse MWH, Merkx M, Averill BA (1999) Biochemistry 38:9926–9936
42. Wang XD, Ho RYN, Whiting AK, Que L Jr (1999) J Am Chem Soc 121:9235–9236
43. Smoukov SK, Quaroni L, Wang X, Doan PE, Hoffman BM, Que L Jr (2002) J Am Chem Soc 124:2595–2603
44. Griffith JP, Kim JL, Kim EE, Sintchak MD, Thomson JA, Fitzgibbon MJ, Fleming MA, Caron PR, Hsiao K, Navia MA (1995) Cell 82:507–522
45. Davis JC, Lin SS, Averill BA (1981) Biochemistry 20:4062–4067
46. Vogel A, Spener F, Krebs B (2001) In: Messerschmidt A, Huber R, Poulos T, Wieghardt K (eds) Handbook of metalloproteins. Wiley London
47. Vincent JB, Crowder MW, Averill BA (1991) Biochemistry 30:3025–3034
48. True AE, Scarrow RC, Randall CR, Holz RC, Que L Jr (1993) J Am Chem Soc 115:4246–4255
49. Day EP, David SS, Peterson J, Dunham WR, Bonvoison JJ, Sands RH, Que L Jr (1988) J Biol Chem 263:15561–15567
50. Dietrich M, Münstermann D, Suerbaum H, Witzel H (1991) Eur J Biochem 199:105–113
51. Averill BA, Davis JC, Burman S, Zirino T, Sanders-Loehr J, Loehr TM, Sage JT, Debrunner PG (1987) J Am Chem Soc 109:3760–3767
52. Ek-Rylander B, Barkhem T, Ljusberg J, Ohman L, Andersson KK, Andersson G (1997) Biochem J 321:305–311
53. Antanaitis BC, Aisen P (1982) J Biol Chem 257:1855–1859
54. Davis JC, Averill BA (1982) Proc Natl Acad Sci USA 79:4623–4627
55. Rusnak F, Mertz P (2000) Physiol Rev 80:1483–1521
56. Mertz P, Yu L, Sikkink R, Rusnak F (1997) J Biol Chem 272:21296–21302
57. Hoff RH, Mertz P, Rusnak F, Hengge AC (1999) J Am Chem Soc 121:6382–6390
58. Hengge AC, Martin BL (1997) Biochemistry 36:10185–10191
59. Martin BL, Graves DJ (1994) Biochim Biophys Acta 1206:136–142
60. Christianson DW, Cox JD (1999) Annu Rev Biochem 68:33–57
61. Funhoff EG, Wang Y, Andersson G, Averill BA (2005) FEBS J 272:2968–2977
62. Wang X, Que L Jr (1998) Biochemistry 37:7813–7821
63. Klabunde T, Sträter N, Fröhlich R, Witzel H, Krebs B (1996) J Mol Biol 259:737–748
64. Egloff MP, Cohen PTW, Reinemer P, Barford D (1995) J Mol Biol 254:942–959
65. Dikiy A, Funhoff EG, Averill BA, Ciurli S (2002) J Am Chem Soc 124:13974–13975
66. Kissinger CR, Parge HE, Knighton DR, Lewis CT, Pelletier LA, Tempczyk A, Kalish VJ, Tucker KD, Showalter RE, Moomaw EW, Gastinel LN, Habuka N, Chen X, Maldonado F, Barker JE, Bacquet R, Villafranca JE (1995) Nature 378:641–644
67. Todd MJ, Hausinger RP (2000) Biochemistry 39:5389–5396
68. Pohjanjoki P, Fabrichniy IP, Kasho VN, Cooperman BS, Goldman A, Baykov AA, Lahti R (2001) J Biol Chem 276:434–441

69. Chen GJ, Edwards T, Dsouza VM, Holz RC (1997) Biochemistry 36:4278–4286
70. Harris MN, Ming LJ (1999) FEBS Lett 455:321–324
71. Kawabe H, Sugiur Y, Terauchi M, Tanaka H (1984) Biochim Biophys Acta 784:81–89
72. O'Hara A, Sawada H, Kato T, Nakayama T, Yamamoto H, Matsumoto Y (1984) J Biochem 95:67–74
73. Wang X (1998) PhD Dissertation, University of Minnesota
74. Merkx M, Averill BA (1998) Biochemistry 37:8490–8497
75. Merkx M, Averill BA (1999) J Am Chem Soc 121:6683–6689
76. Gehring S, Fleischhauer P, Behlendorf M, Hüber M, Lorösch J, Haase W, Dietrich M, Witzel H, Löcke R, Krebs B (1996) Inorg Chim Acta 252:13–17
77. Merkx M, Averill BA (1998) Biochemistry 37:11223–11231
78. Martin RB (1988) In: Sigel H (ed) Metal ions in biological systems 24. Marcel Dekker Inc, pp 1–57
79. Kido H, Saito K (1988) J Am Chem Soc 110:3187–3190
80. Funhoff EG, Bollen M, Averill BA (2004) J Inorg Biochem 99:521–529